

Growth of Li-B nanocrystals on the Surface of LiF Laser Crystal at 60Co Gamma-Irradiation



E M Ibragimova^{1,2*}, Sh N Buzrikov¹, N E Iskandarov², M A Mussaeva¹ and Kh T Nazarov²

¹Institute of nuclear physics, Academy of sciences, Uzbekistan

²Center for advanced technologies, Ministry of innovation development, Uzbekistan

Submitted: October 25, 2021; Published: December 03, 2021

*Corresponding author: E M Ibragimova, Institute of nuclear physics, Academy of sciences, Center for advanced technologies, Ministry of innovation development, Tashkent, Uzbekistan

Abstract

This work was aimed at studying structure-phase transformations in passive laser Q-switch made of LiF:OH, interfaces and nanoparticles, grown at exposure to isotropical ⁶⁰Co-γ-quanta flux to the doses 10⁷-10⁸ R, combining SEM, SPM, XRD, UV-vis and FTIR techniques. The origin crystal contains Li and LiH nanophases, and after the irradiation at 273 K low symmetric LiBH phases with larger lattice parameters can grow only on the surface as separated hillocks, while at 320 K atom diffusion allows to assemble a wall of these phases. Optical spectra contain both absorption and scattering centers with the ratio depending on the irradiation temperature. Oxygen could have come from air. The only origin of so many atoms of B and H and more Li is a special nuclear branching decay ¹⁹F₉+γ→¹¹B₅+⁷Li₃+¹H₁ under absorption of 1.17 and 1.33 MeV γ-quanta by F-nuclei. Another way is nuclear compound transmutation ¹³(HLiF)²⁷+γ→¹³(BO)²⁷→⁵B¹¹+⁸O¹⁶.

Keywords: Nanophases; Irradiation with gamma-quanta; Decay of light nuclei; Optical absorption; Light scattering

Introduction

Being the widest gap (14 eV) ionic dielectrics, LiF crystals have attracted much attention and various applications as dosimeters and detectors of ionizing radiation in wide energy range [1,2], and the novel high contrast radiation imaging detector [3-6]. Besides, LiF after gamma-irradiations to doses 10⁷-10⁸ R can operate as room temperature cw tunable and passive nano-picosecond laser Q-switch [7-9]. The radiation effect was ascribed to saturated absorption of shallow F₂ color centers each trapping and releasing an electron at the picosecond rate. Besides generation of primary neutral F-H and charged α-I pair defects, Li metallic colloids are known to grow during long term irradiation by means of aggregation of anion vacancies in bubbles and interstitial cations in colloids by slow diffusion process [10-15] and may limit the operation resource of laser device. The important role of H and OH impurity centers in non-linear effects was noted in [7,16]. Phase transformations also take place under irradiation by mechanisms of ballistic transport and radiation-enhanced diffusion and influence the properties [17]. Possible effects of electron-positron pairs and nuclear reactions produced by γ-quanta on phase transformations were not considered [18]. The opinion that

«ionizing irradiations of LiF cause radiolysis with F release from the surface» was proved by generation of anion vacancies and their aggregates and based on assumption of decay of localized excitons into defects [7-16]. However, this decay model did not consider / explain what kind of nuclear moment expels F ion from its site and why lighter Li ions are not expelled by the nuclear excitation and instead assemble in colloids. Optical response of metal clusters was proved to differ from electron oscillators [19,20]. Recently we found that undoped LiF has nanophase of LiH and Li₂O, and after ⁶⁰Co-γ- and electron- irradiations Li metal grow as ordered micro-nano-strips [21], which cause strong light scattering according to G Mie theory rather than optical absorption by point defects [19].

This work was aimed at studying structure-phase transformations in LiF:OH single crystal under exposure to intensive γ-quanta flux and optical response of interfaces between LiF matrix and Li and other nanoparticles grown there.

Samples and Experiment

LiF crystals doped with OH were grown, cut and polished at State Optical Institute (St. Petersburg, Russia). The laser element

bars 15×15×40 mm ($V=9 \text{ cm}^3$) were irradiated at INP AS RUz with ^{60}Co - quanta ~ 1.17 and 1.33 MeV in isotropic 4π -geometry chamber to exposure doses 10^7 - 10^8 R at the dose rate 1100 R/s in ice at 273 K and at 150 R/s in dry air at 320 K. The integral γ -fluency passing through the sample surface reached 10^{18} cm^{-2} , so each atom of the dense LiF lattice could absorb one γ -quant. These conditions turned out optimal for performing either the tunable laser or the passive laser Q-switch in NIR range [7-9]. The samples of 2mm thick were cut from the expired (20 years) active and passive laser elements for the experiments.

A few surface-sensitive techniques were implemented to separate contributions from surface and bulk defects especially important in the case of large laser elements. Absorption and reflection spectra were measured in the wavelength range 190-3000nm at the spectrophotometers double beam UV3600 (Shimadzu) and single beam SF-56 (LOMO), having the opposite scan directions between UV and IR to take into account possible excitation of luminescence. Vibration spectra were measured

at FTIR spectrometer iS50 Nicolet (Thermo Scientific) in the wave number range 4000-400 cm^{-1} (resolution 1 cm^{-1}) using transmission and attenuated total reflection modes so as to reveal the contribution from irradiated surface. Crystal structure was determined at X-ray diffraction spectrometer Epyrean (P Analytical) with a pixel detector in the angle range 5-130 grad and by Full Prof code, phase analysis used PDF-2 data. Surface topology was studied at scanning probe microscope SPM-9700HT (Shimadzu) and scanning electron microscope EVO MA10 (Zeiss), local element analysis was done with EDS-energy dispersion system AZtex INCA (Oxford Instrum.).

Results and Discussion

The experiments began from observation of surface microstructure and local element composition of LiF:OH samples, which were ^{60}Co γ -irradiated to the dose of 10^8 R at temperatures at 270 K (when Li interstitials are immobile), 320 and 350K (when Li interstitials and anion defects are mobile), as represented in Figures 1 & 2 below.

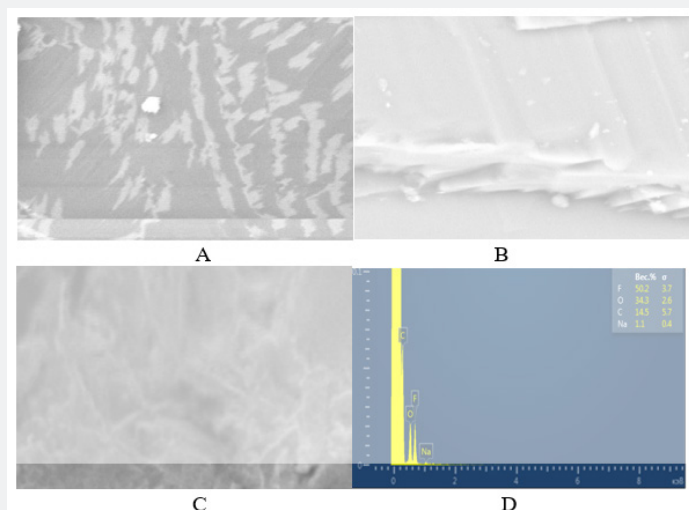


Figure 1: SEM for LiF:OH ^{60}Co -irradiated to 10^8 R at temperatures: A-350 K, image area $20 \times 20 \mu\text{m}$ coated with 20 nm graphen; B- 273 K, $50 \times 50 \mu\text{m}$; C- 320K, $50 \times 50 \mu\text{m}$ and D-EDS of the surface shown in (C).

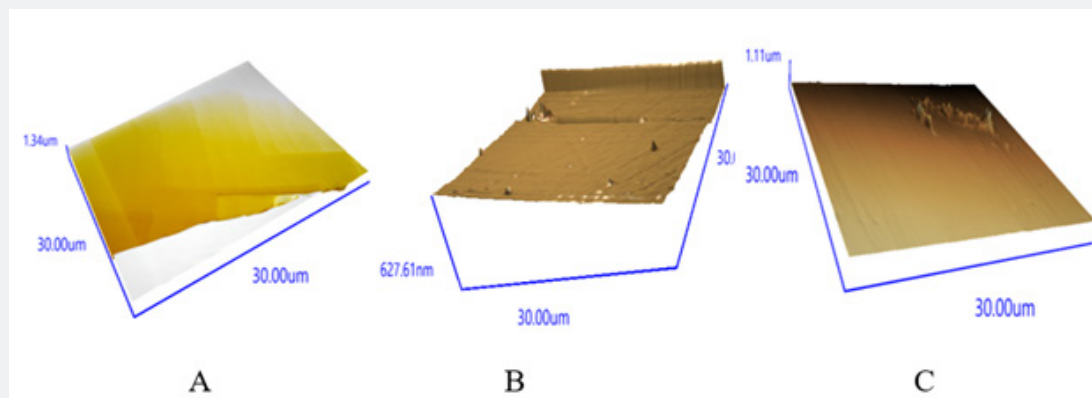


Figure 2: SPM of LiF:OH surface of the pristine (A) and irradiated to dose 10^8 R at 273 K (B) and 320 K (C), scanned in non-contact mode.

EDS spectrum of the non-irradiated LiF (not coated with Carbon) contains only single K-emission line of Fluorine. Broad intensive K-emission below 0.4keV includes unresolved lines of Li, B and C. Bright spots and stripes are enriched with Li and LiBH-compounds conducting electric current. Figure 2A shows smooth non-irradiated surface with straight cleaved steps. After intensive irradiation in ice (Figure 2B) one can see only a few nano-cones of ~60nm height separated ~15μm on the flat surface. While a cycle

of many nano-cones is formed at the linear defect. But after dry irradiation at 320 K all mobile interstitials easily formed a round wall (Figure 2C).

These XRD spectra demonstrate that ⁶⁰Co γ-irradiation is not homogeneous on/in the laser switch of 9 cm³ bulk and it cannot penetrate LiF without losses. The results of structure and phase analysis of these spectra are listed in Table 1 below.

Table 1: Structure analysis and phase composition of LiF:OH.

Phase	v.%	Group	a, nm	b, nm	c, nm
Non-irradiated sample (spectrum 1) inside cleaved surface					
LiF	48	Fm-3m	0.4035	0.4035	0.4035
Li	13	Fm-3m	0.39	0.39	0.39
LiH	39	Fm-3m	0.40841	0.40841	0.40841
60-Co gamma-irradiation at 1100 R/s to 100 MR at 273 K (sp.3) inside surface					
LiF	3	Fm-3m	0.403	0.403	0.403
Li	5	Fm-3m	0.4389	0.4389	0.4389
(LiF) ₂ (B ₂ O ₃) ₃	15	Cc	0.48211	1.6149	1.0057
Li(BH ₄)	7	Pnma	0.71914	0.44256	0.68641
Li(BH ₂)	52	Pnma	0.81	0.3	0.59
B	14	R-3m	1.0925	1.0925	2.3814
LiOH	4	P4/nmm	0.3557	0.3557	0.4339
60-Co gamma-irradiation at 150 R/s to 100 MR at 320 K					
LiF	56	Fm-3m	0.405	0.405	0.405
Li	6	R-3m	0.24023	0.24023	0.55159
LiH	12	Fm-3m	0.41	0.41	0.41
B ₂ O ₃	1	P3121	0.43359	0.43359	0.83426
LiOH	1	P4/nmm	0.3549	0.3549	0.4334
LiO ₂	1	Pnnm	0.3992	0.4877	0.2961
(LiF) ₂ (B ₂ O ₃) ₃	3	Cc	0.48211	1.6149	1.0057
Li(BH ₄)	14	Pnma	0.71914	0.44256	0.68641
Li(BH ₂)	2	Pnma	0.81	0.3	0.59
B	3	P42/nmm	0.8708	0.8708	0.5075
F ₂	1	C2/m	0.55	0.328	1.001

The pristine surface (spectr. 1) contains only cubic LiF, Li and LiH phases with close lattice parameters (difference ~0.01 nm), therefore it has smooth coherent interfaces (Figure 2A). After γ-irradiation at 273 K (Figure 2B) low symmetric LiBH phases with larger lattice parameters can grow only on the surface as separated hillocks. While at 320 K diffusion allows to assemble a wall (Figure 2C). Using well-known Scherrer formula [17] we calculated for the pristine crystal the size of structure domains of LiF matrix, which is 160-180nm, and for LiH, which is 105nm. After the irradiation at 273K the sizes of grown Li (BH₂), (LiF)₂(B₂O₃)₃ and B phases are 210-220 nm, while the size of LiF domain decreased

to 100-120nm, and new Li phase appeared with larger lattice parameters and small sizes ~5nm (colloidal size [11,13,17,19]). Nanoparticles < 5nm were estimated from the diffuse band at low angles 10-30 grad, weak selective reflexes at larger angles aside the dominant matrix reflections were attributed to nanocrystals of < 30nm thick. Narrow high (>10⁵ counts) peaks at 45 and 100 grad with broad foot ±5 grad below 10³ counts characterize lattice deformation due to rod-like nanoparticles (model shape 5×50nm) grown on a crystal substrate (Figure 2b & 2c). There is no such broadening only on the relaxed outside surface of pristine crystal with coherent interfaces (see spectrum 3 in Figure 3).

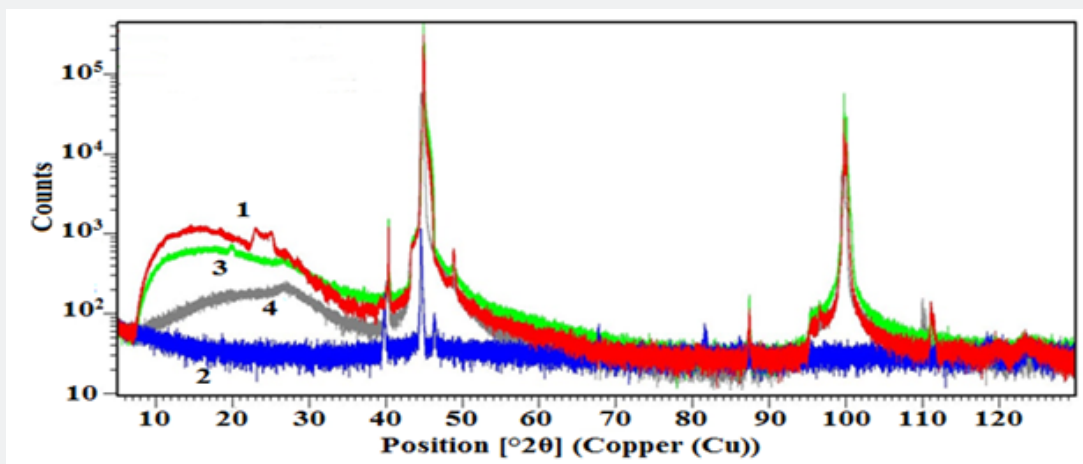


Figure 3: XRD spectra of rotating LiF:OH non-irradiated (1,2) and after 60Co γ -irradiation to 10⁸ R at 273 K (3,4), registered from outside (2,4) and inside (1,3) cut surfaces.

Data listed in Table 1 demonstrate that the same dose 10⁸ R accumulated at 7 times less dose rate and a higher temperature of 320 K resulted in some recovery of LiF phase, although 3 times decreased LiH, 2 times Li, and generated 14% Li (BH₂) phase and 7 more tiny phases with Li, B, O, H. Oxygen could have come from air. The only origin of so many atoms of B and H and more Li is a special nuclear branching decay $^{19}\text{F}_9 + \gamma \rightarrow ^{11}\text{B}_5 + ^7\text{Li}_3 + ^1\text{H}_1$ under absorption of 1.17 and 1.33 MeV γ -quanta by F-nuclei. Another

way is nuclear compound transmutation:



Figure 4 shows optical absorption and reflection spectra of LiF:OH (A and B were scanned at single beam SF-56, C and D were scanned at double beam UV3600 spectrophotometer) prior and after gamma-irradiations to the large range of exposure doses and the temperatures mentioned above in Figures 1-3 & Table 1.

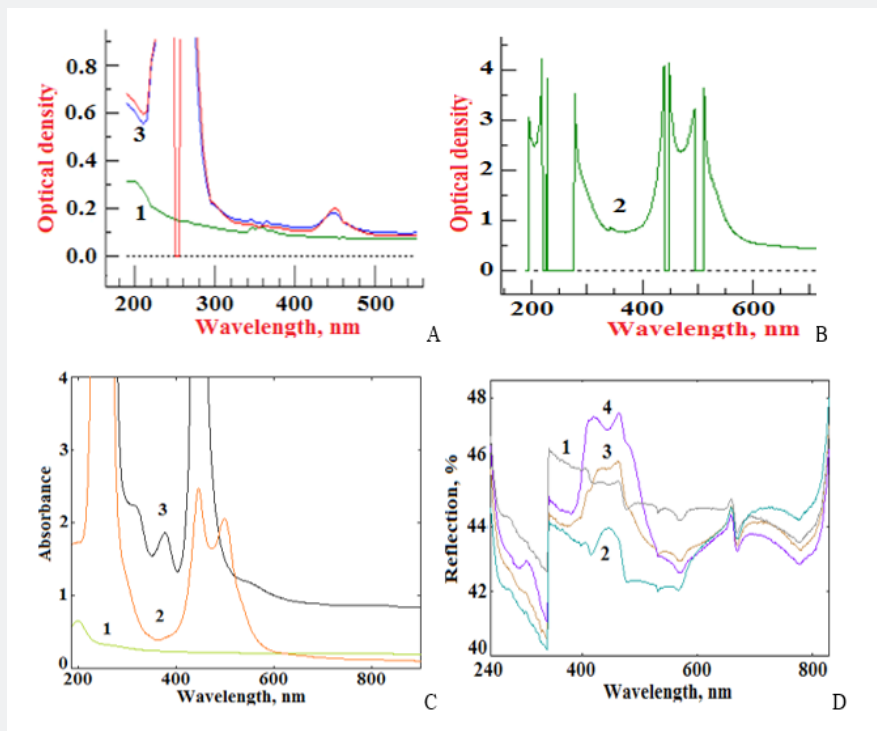


Figure 4: Spectra of LiF:OH 2 mm: all 1 correspond to the pristine sample, 2-4- after γ -doses: absorption A) 2- 6 \times 10⁵ R, 3- 7 \times 10⁵ R at 320 K; (B) 10⁸ R at 273 K; (C) 10⁸ R at 2- 273 K, 3- 350 K; and reflection (D) 10⁸ R at 2- 273 K, 3- 320 K, 4- 350 K.

Spectra (1) in Figure 4a-4d for non-irradiated (pristine) sample scanned in the absorption and reflection modes have unresolved bands at 200 and 260 nm and 340-380nm, which are related with impurity nano-phases scattering the incident light, rather than absorbing or reflecting it [19,20]. After gamma-irradiation to the dose 7×10^5 R the absorption band at 250nm of the known F-center saturates and split, when the nearest F-centers approach to the distance of interaction estimated ~ 14.5 nm and form *F-F* dipole (corresponding spectrum 3a). At this moment there appears a weak band at 450 nm ascribed to molecular M or (F₂), which after saturation at the dose $< 10^8$ R form M-M dipole at the distance ~ 22 nm with split doublet 440 and 500 nm (spectra 2b,2c,3c,3d,4d). Spectra 2b and 2c of samples irradiated to 10^8 R in ice at 273K to avoid Li-colloids indeed have no bands at 370 and 520nm [8-10]. The split bands do not have Gaussian profile therefore they cannot be attributed to single electron oscillators according to the Smakula model [10,11,16]. Zero absorbance corresponds to zero dielectric permittivity $\epsilon=0$ [22], but this 0-band (with the width increasing with gamma-dose from 3a to 2b) is between very intensive scattering resonances. Reflection at the same wavelength as absorption of M-centers at 450nm cannot be attributed to this point defect, but evidences on assembling metal colloid from the point defects. Weak wide absorption bands at 380, 520 and 700nm were attributed to plasmon response of Li containing nanocrystals of elongated shape [19]. It was

established that appreciable enhancement of absorption occurs when the length of free electron path is larger but comparative with the nano-particle size [19,20].

Zero-epsilon photonic bands appear around the maximum wavelength of F- and M-bands at 245 and 445 nm respectively [20,22], after their intensities get saturated and split to doublet (Figure 2A spectra 2 and 3). Simultaneously reflection at the photonic band increases (Figure 2B spectra 2-3-4, it means there is no absorption within the band).

Figure 5 shows IR vibration spectra of non-irradiated and gamma-irradiated LiF:OH registered in both transmission and reflection modes so as to compare the bulk and surface response, respectively. The spectrum 1 of non-irradiated sample (Figure 5a & 5b) contains Li-F stretching at 1000 cm^{-1} and bending overtone at 700 cm^{-1} ; Li-Li at 500 cm^{-1} ; OH-groups at $3720\text{-}3550 \text{ cm}^{-1}$; LiH triplet at $2850\text{-}2920\text{-}2970 \text{ cm}^{-1}$. The irradiation induced band at 2000 cm^{-1} is attributed to stretching of B-O bond from impurity Boron oxide phase [23]. Thus, assembled nanoparticles are responsible for intensive band at 2000 cm^{-1} and basic absorption shift from 1000 cm^{-1} to 1250 cm^{-1} . Thus, FTIR data agree with XRD phase analysis. FTIR transmission shows, that after γ -irradiation intensive band at 2000 cm^{-1} and weak broad bands are related to B and O containing phases.

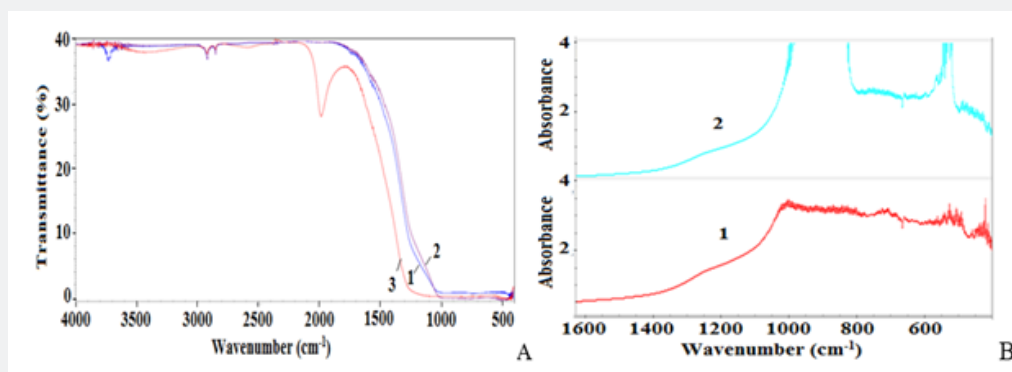


Figure 5: FTIR spectra of LiF:OH: (a) transmission of (1) non-irradiated, ^{60}Co -gamma-irradiated to 10^8 R at 273 K (2) and 350 K (3); (b) reflection of non-irradiated (1) and irradiated at 273 K (2).

Figure 6 demonstrates a simplified model of possible close packed composite nanostructure, where white ~ 100 nm LiF cubs are laid with black Li and LiH bars of 17nm (estimated from XRD), which we suggested for describing the subsurface layer of LiF:OH type of optic material for lasers. But both phases have the same cubic symmetry and very close lattice parameters (Table 1).

After gamma-irradiation the dominating impurity LiBH phases grew to 27nm. Besides, these phases have low symmetry and significant difference in lattice parameters, therefore they cannot maintain coherent interfaces with cubic LiF matrix. Such a nano-structural composite can operate as 3D phase grating in passive

nano-picosecond laser Q-switch [7-9]. Simple oxide phases and complicate $(\text{LiF})_2(\text{B}_2\text{O}_3)_3$ grow as nanofilms on the surface, like many other cases [17].

Conclusion

Thus, combining SEM, SPM, XRD, UV-vis and FTIR techniques phase transformations can be studied carefully. Lithium as the lightest metal could not be detected directly by EDS at SEM and the characteristic X-ray spectra contained mostly F and some oxygen. Since Li has the highest electron density, it is possible to observe the bright contrast in SEM and ascribe it to electric

conducting Li-B-H containing nanophases. According to XRD, impurity nanophases giving weak reflections aside the weakened and broadened basic reflections of LiF, are attributed to LiH, Li₂O, existed in non-irradiated LiF, and also LiF-B₂O₃ and LiBH appeared after intensive long term irradiation. The interfaces between LiF crystal matrix and Li containing nanoparticles are ordered and coherent, so the irradiations result in formation of nanocomposite in the subsurface layer of tens microns. The complex compound of Li halide, Li₂O and BO₃ is the best superionics [23]. The dose-rate and irradiation time and also the irradiation temperature control the structure-phase composition and hence the optical spectra. Optical absorption and reflection allow separate point color centers from metal colloids. Only FTIR spectra in the reflection mode could show the significant weakening of Li-F stretch vibration and increasing of Li-Li vibration after irradiations. The

irradiations to heavy dose of 100 MR with ⁶⁰Co γ-quanta 1.17 and 1.33 MeV of LiF cause F nuclear fission rather than radiolysis with F release from the surface [6-15]. It is the primary reason for following heterogeneous nucleation of the impurity nanophases with participation of stable products of nuclear reactions in the expired passive shutter. When the g-flux is so intensive that can excite simultaneously odd nuclei ¹H¹⁺, ³Li⁷⁺, ⁹F¹⁹ in very dense ionic lattice with overlapped electron shells at interatomic distance 0.1nm in LiH and 0.2nm in LiF, they can fuse in a short living compound ¹³(HLiF)²⁷ which transforms to another compound ¹³(BO)²⁷ followed by decay (fission) into stable odd ⁵B¹¹ and even ⁸O¹⁶ nuclei. Also, possible branching decay of ¹⁹F₉ + γ → ¹¹B₅ + ⁷Li₃ + ¹H₁ all stable isotopes produce chemical compound LiBH determined by XRD as a dominating phase [24].

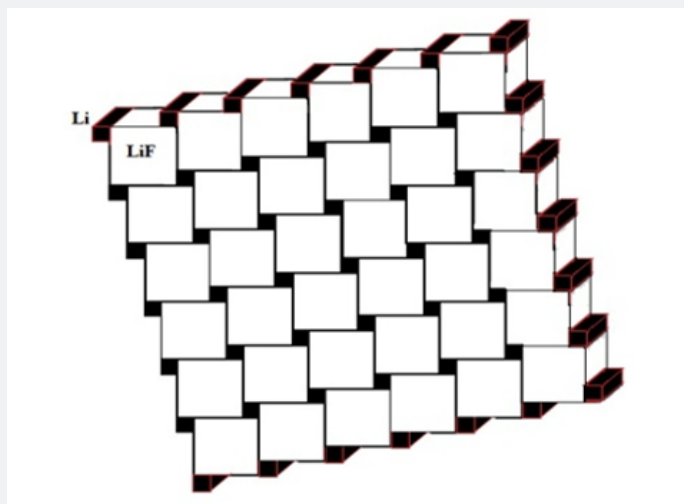


Figure 6: Model of ordered LiBH-nanophase separating the basic LiF phase.

Funding

The research was supported by Programme under President Degree 4526.

References

- Baldacchini G (2002) Colored LiF: an optical material for all seasons. *J of Lumin* 100: 333-334.
- R Kopec, Closowski M, Liszka M (2013) The dose and X-ray energy response of LiF:Mg,Cu,P and CaSO₄:Dy thermoluminescent foils. *Radiat Measur* 56: 380-383.
- Montealeali RM, Bonfigli F, Piccinini M, Nichelatti E, Vincenti MA (2016) Photoluminescence of color centers in lithium fluoride thin films: from solid-state miniaturized light sources to novel radiation imaging detectors. *J Lumin* 170: 761-769.
- Bilski P, Marczevska B, Gieszczyk W, Kłosowski M, Nowak T, et al. (2018) Lithium fluoride crystals as fluorescent nuclear track detectors. *Radiation Protection Dosimetry* 178(3): 337-340.
- Bilskia P, Marczevskaa B, Gieszczyka W, Kłosowska M, Naruszewicz M, et al. (2019) *Journal of Luminescence* 213: 82-87.
- Estrela P, Maçôas E, Williams G, Hussain M, Fajardo M (2021) Lithium fluoride detectors for high spatial resolution imaging of tabletop XUV from high harmonic generation in gases. *Journal of the Optical Society of America B* 38(7): 2234-2238
- Mollenauer LF, Stolen RH, Gordon JP (1980) Experimental Observation of Picosecond Pulse Narrowing and Solitons in Optical Fibers. *Optic Letters* 5, 188 *Phys Rev Lett* 45: 1095.
- Basiev TT, Mirov SB, Osiko VV (1988) Room-temperature color center lasers. *IEEE J Quant Electron* 24(6): 1052-1069.
- Ter-Mikirtychev VV, Tsuboi T (1996) Stable room-temperature tunable color center lasers and passive Q-switchers. *Prog Quant Electron* 20(3): 219-268.
- Shwartz KK, Lyushina AF, Vitol AY (1969) *Solid State Phys* 11: 1885.
- Jain U, Lidiard AB, (1977) *Philos Mag* 35: 245-259.

12. Dubinko VI, Turkin AA, Vainstein DI, den Hartog HW (2000) Theory of the late stage of radiolysis of alkali halides. *J Nucl Mater* 277: 184-198.
13. Beuneu F, Vaida P, Zogal OJ (2002) *NIMB* 191: 149-153.
14. Izerrouken M, Souami N, Guerbous L, Djaroum S, Kadouma M, et al. (2008) Li colloids formation study induced by reactor neutrons in LiF single crystals. *NIMB* 266(12-13): 2745-2749.
15. Bryukvina LI, Martynovich EF (2012) Formation and properties of metallic nanoparticles in lithium and sodium fluorides with radiation-induced color centers. *NIMB* 54(12): 2374-2378.
16. AV Erganov (1993) *Phys stat.sol (b)* 179: 323-327.
17. Wollenberger H (1994) *J Nucl Mater* 216: 63-77.
18. Hubbell JH (2006) Electron-positron pair production by photons: a historical overview. *Radiat Phys and Chem* 75(6): 614-623.
19. Kriebig U, Vollmer M (1995) Effect of Substrate Temperature on Structural and Optical Properties of Au/SiO₂ Nanocomposite Films Prepared by RF Magnetron Sputtering. *Optical Properties of Metal Clusters*, (Springer-Verlag), Berlin, Germany.
20. Klimov VV (2014) *Nanoplasmonics*. Pan Stanford, Singapore.
21. Ibragimova EM, Mussaeva MA (2019) Electron Microscopy and Elemental Composition of the Near-Surface Layer of Electron-Irradiated LiF Crystals. *Technical Physics Letters* 45(2): 155-158.
22. Robert Boyd (2021) *Nonlinear Optical Processes in Epsilon-near-zero Materials*. FiOLS. Univ Ottawa, Canada.
23. Jak JG, Kelder EM, Schoonman J (1999) *Solid State Ion* 142: 74.
24. Dolling G, Smith HG, Nicklow RM, Vijayaraghavan PR, Wilkinson MK (1968) Lattice Dynamics of Lithium Fluoride. *Phys Rev* 168(3): 970.



This work is licensed under Creative Commons Attribution 4.0 License
DOI: [10.19080/JOJMS.2021.06.555695](https://doi.org/10.19080/JOJMS.2021.06.555695)

Your next submission with JuniperPublishers will reach you the below assets

- Quality Editorial service
- Swift Peer Review
- Reprints availability
- E-prints Service
- Manuscript Podcast for convenient understanding
- Global attainment for your research
- Manuscript accessibility in different formats
(Pdf, E-pub, Full Text, Audio)
- Unceasing customer service

Track the below URL for one-step submission

<https://juniperpublishers.com/submit-manuscript.php>